JOURNAL OF SOLID STATE CHEMISTRY 68, 247–254 (1987)

Magnesium and Zinc Cation Distributions and Correlation with Curie Temperature in Some $LiTaO_3$-Based Ferroelectric Ceramics

GI-TAE JOO, J. SENEGAS, J. RAVEZ,* AND P. HAGENMULLER

Laboratoire de Chimie du Solide du CNRS, Université de Bordeaux I, 351, cours de la Libération, 33405 Talence Cedex, France

Received June 9, 1986

Nonstoichiometric ferroelectric ceramics based on $LiTaO_3$ have been sintered at relatively low temperature. The corresponding phases belong to the Li_2O–Ta_2O_5–MO (M = Mg, Zn) systems. A correlation between the calculated electric field gradient seen by Li nuclei and the quadrupole splitting of ^7Li NMR line shape allows the authors to localize the Mg or Zn atoms in either the octahedral or tetrahedral sites of the crystalline network. These results have been correlated to the corresponding Curie temperatures determined in parallel by dielectric measurements. © 1987 Academic Press, Inc.

Introduction

$LiTaO_3$ is a widely used material due to its piezoelectric, pyroelectric, and electrooptical properties and with a relatively high Curie temperature (t_C = 680°C) (*1*). The structure of the ferroelectric $LiTaO_3$ phase has been investigated by Abrahams and coworkers: the symmetry is trigonal with space group $R3c$ (ferroelectric) or $R\bar{3}c$ (paraelectric) (Fig. 1) (*2, 3*). The structure is of the ordered corundum type (α-Al_2O_3) (Fig. 2). The Li and Ta atoms occupy two-thirds of the face-sharing octahedral sites in the hexagonal close-packed oxygen sublattice along the c-axis.

It has been found that the ferroelectric properties can be modulated by partial cationic substitution in $LiTaO_3$ (*4*). The Curie temperature of $LiTaO_3$-type solid solutions increases or decreases generally depending upon the substituting cation localized in either the octahedral or tetrahedral sites of the lattice (Fig. 2) (*5–9*). Some authors have discussed such types of coordination by ^7Li nuclear magnetic resonance (NMR) in $LiTaO_3$-type nonstoichiometric phases substituted partially by Ti^{4+} or Zr^{4+} cations (*9, 10*). They have also tried to relate the t_C variation to the localization of the substituting cation.

Crystal Chemistry

Mg- or Zn-substituted solid solutions derived from $LiTaO_3$ have been prepared by solid state reaction of oxides or carbonates (reagent grade Li_2CO_3, $MgCO_3$, ZnO, and Ta_2O_5). After mixing, the materials were calcined at 800°C for 15 hr or at 900°C for 3 hr to eliminate CO_2 and to improve the sintering properties. The obtained white ceramics were then ground and pelletized as

*Author to whom correspondence should be addressed.

0022-4596/87 $3.00

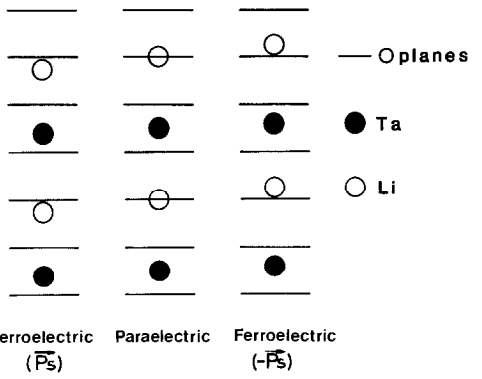

FIG. 1. Cationic shifts along the c-axis at the ferroelectric ($R3c$)–paraelectric ($R\bar{3}c$) t_C transition in $LiTaO_3$.

disks 8 or 13 mm in diameter and about 1 mm in thickness, and then sintered 15 hr at 1200°C.

The phases were identified by X-ray diffraction using Ni-filtered Cu$K\alpha$ radiation. Pure silicon powder was added as an internal standard. Calculation of the lattice parameters was carried out using a least-squares method.

An X-ray diffraction study characterized $LiTaO_3$-type solid solutions in the Li_2O–Ta_2O_5–MgO or Li_2O–Ta_2O_5–ZnO diagrams. Formulas, solid solution limits, lattice parameters, and c/a axial ratios are reported in Table I.

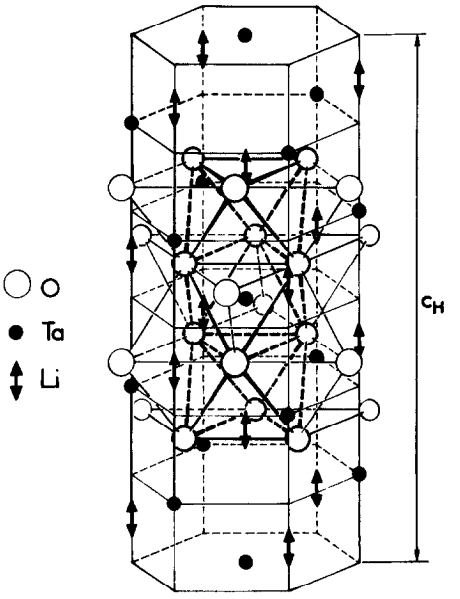

FIG. 2. Schematic view of the $LiTaO_3$ structure.

Dielectric Measurements

Dielectric measurements were performed at 1 kHz from room temperature to 850°C with an automatic capacitance bridge (Wayne-Kerr, B905) on sintered ceramic disks. Gold electrodes were deposited on circular faces by cathodic sputtering.

For each composition a maximum of the permittivity ε_r' is associated with a mini-

TABLE I

FORMULAS, LATTICE PARAMETERS, AND BORDER PHASE CURIE TEMPERATURE OF THE STUDIED $LiTaO_3$-TYPE SOLID SOLUTIONS

System	Formula	Number of cations per unit formula	γ, stoichiometry deviation for unit formula	Approximately upper limit of x	Upper limit of γ for x_{max}	Lattice parameters for border phase			t_C for border phase (°C)
						a_H (Å)	c_H (Å)	c/a	
Li_2O–Ta_2O_5–MgO	$Li_{1-x}Mg_{3x}Ta_{1-x}O_3$	$2+x$	$+x$	0.1	0.1	5.1551	13.8138	2.680	700
	$Li_{1-x}Mg_{4x/3}Ta_{1-x/3}O_3$	2	0	0.2	0	5.1545	13.8044	2.678	730
	$Li_{1-x}Mg_{x/2}TaO_3$	$2-x/2$	$-x/2$	0.3	−0.15	5.1588	13.7977	2.675	710
Li_2O–Ta_2O_5–ZnO	$Li_{1-x}Zn_{3x}Ta_{1-x}O_3$	$2+x$	$+x$	0.05	0.05	5.1582	13.7793	2.671	610
	$Li_{1-x}Zn_{4x/3}Ta_{1-x/3}O_3$	2	0	0.4	0	5.1695	13.8231	2.674	520
	$Li_{1-x}Zn_{x/2}TaO_3$	$2-x/2$	$-x/2$	0.5	−0.25	5.1737	13.7908	2.666	460

mum of the dielectric losses tan δ at the ferroelectric Curie temperature. Figure 3 shows, as an example, the thermal dependence of ε_r' and tan δ for $Li_{0.900}Zn_{0.133}Ta_{0.967}O_3$ composition. The values of the Curie temperature t_C for the border phase of each solid solution are given in Table I. Figure 4 shows the t_C variation of each solid solution with increasing x. The Curie temperature, compared with that of $LiTaO_3$, increases for Mg-containing solid solutions and decreases for Zn-containing ones. The border composition $Li_{0.50}Zn_{0.25}TaO_3$ which is cation deficient, has the lowest Curie temperature (t_C = 460°C). Such behavior had previously been observed for the $LiTaO_3$–$MTiO_3$ (M = Mg, Zn) systems (*11*).

NMR Investigation

NMR measurements on ^7Li nuclei were performed for ceramic samples at 14 MHz (8.47 kG) for the temperature range between −60 and 180°C. No thermal variation was observed for any spectrum over this temperature interval. The continuous-wave spectrometer was coupled to a magnet giving a magnetic field homogeneity of $\Delta H/H \leq 10^{-5}$ over the sample. Two modulating fields (H_m = 0.72 and 2.4 G) were used successively to evaluate the influence of the detection technique on the shape and width of the resonance lines.

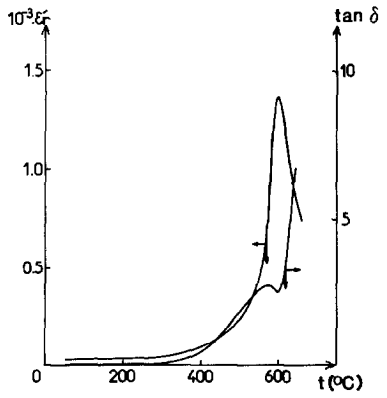

FIG. 3. Thermal dependence of ε_r' and tan δ for a ceramic with composition $Li_{0.900}Zn_{0.133}Ta_{0.967}O_3$ (at 1 kHz).

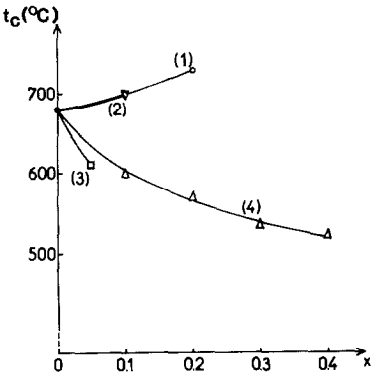

FIG. 4. Variation of Curie temperature with x for ceramic compositions: (1) $Li_{1-x}Mg_{3x}Ta_{1-x}O_3$; (2) $Li_{1-x}Mg_{4x/3}Ta_{1-x/3}O_3$; (3) $Li_{1-x}Zn_{3x}Ta_{1-x}O_3$; (4) $Li_{1-x}Zn_{4x/3}Ta_{1-x/3}O_3$.

Lithium has a nuclear spin $I = \frac{3}{2}$ and a quadrupole moment. Its resonance spectrum can split into three lines corresponding to the $-\frac{3}{2} \rightarrow -\frac{1}{2}$, $-\frac{1}{2} \rightarrow +\frac{1}{2}$ and $+\frac{1}{2} \rightarrow +\frac{3}{2}$ transitions. The signal to noise ratio may decrease, requiring a relatively strong modulation field in order to detect the satellites. The corrected second moment $M_{2_{corr}}$ can then be expressed as following (*12*)

$$M_{2_{corr}} = M_{2_{exp}} - \frac{H_m^2}{4},$$

where $M_{2_{exp}}(G^2)$ is the value deduced from experimental spectrum and $H_m(G)$ that of the modulation field. A computer program allows us to determine $M_{2_{exp}}$ from the central line on hand of the relationship:

$$M_{2_{exp}} = \frac{\frac{1}{3}\int_{-\infty}^{+\infty} h^3(h)dh}{\int_{-\infty}^{+\infty} h(h)dh},$$

where h is the algebraic deviation (G) calculated from the resonance field H_0 and $f(h)$ is the derived absorption signal recorded with the synchronous detection system.

A theoretical second moment (G^2) has been calculated with an expression derived

from that of Van Vleck (*13*):

$$M_{2_{th}} = \tfrac{3}{5}\gamma_I^2\hbar^2 I(I+1)N^{-1}\alpha_i^{-1}\sum_{i,j=1}^{N}\alpha_i\alpha_j r_{ij}^{-6}$$

$$+ \tfrac{4}{15}\hbar^2 N^{-1}\alpha_i^{-1}\sum_{i=1}^{N}\gamma_s^2 S(S+1)\sum_{i,k=1}^{N}\alpha_i\alpha_k r_{ik}^{-6}.$$

All terms have their usual meaning, but the parameters α_i, α_j, and α_k (i.e., the occupation rates of the i, j, and k sites) are added to take into account the distribution in the cationic sites. The Abragam (*14*) correction for quadrupole splitting is applied for the central peak, corresponding to the nuclear transition $-\frac{1}{2} \rightarrow +\frac{1}{2}$. The ratio of the second moments in presence and in absence of the quadrupole effect (M_{2_Q}/M_{2_D}) is equal to 0.9 for Li atoms in normal sites (in the case of $LiTaO_3$) and to 0.8 for Li atoms in different sites (i.e., for simultaneous occupation of octahedral and tetrahedral sites by the Li atoms).

All resonance spectra were characterized by a first-order quadrupole effect of ^7Li, $\nu_Q = e^2qQ/2h$, varying from 38 to 44 kHz. An illustration is given for the compositions $LiTaO_3$, $Li_{0.95}Zn_{0.15}Ta_{0.95}O_3$ and $Li_{0.50}Zn_{0.25}TaO_3$ (Fig. 5). Two types of information have been collected and analyzed:

The experimental second moment ($M_{2_{exp}}$) obtained from the central line and corrected by the modulation factor.

The strength of the quadrupole splitting and the width of the satellites, which can be both connected to the cation distribution.

Two hypotheses relative to occupation of the vacant sites by Mg or Zn atoms have been tested:

Hypothesis 1 (H1): simultaneous statistical occupation by Mg (or Zn) atoms of vacant lithium or tantalum sites and of octahedral vacancies of the $LiTaO_3$ structure.

Hypothesis 2 (H2): similar to H1 but Mg (or Zn) atoms, as far as they do not substitute for Li and Ta, now occupy tetrahedral vacancies.

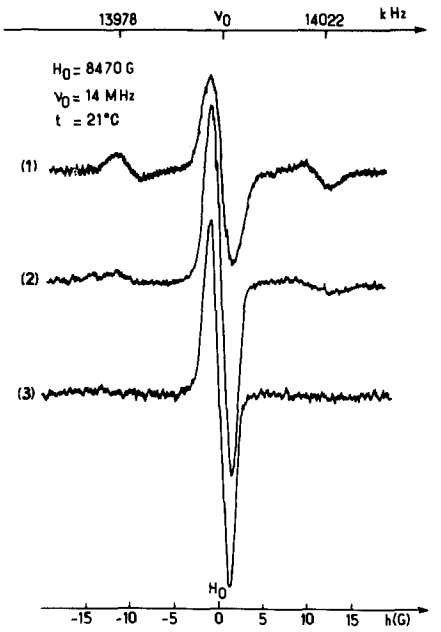

FIG. 5. ^7Li quadrupole splitting for three compositions: (1) $LiTaO_3$; (2) $Li_{0.95}Zn_{0.15}Ta_{0.95}O_3$; (3) $Li_{0.50}Zn_{0.25}TaO_3$.

There are six oxygen layers along the c-axis in a $LiTaO_3$ unit cell. An octahedral site is surrounded by six tetrahedral sites in each layer (Fig. 2) and a tetrahedral one by three octahedral sites. The Mg (or Zn) atoms are supposed to be located at the center of their sites when they occupy the vacant octahedral or tetrahedral sites. The positions of the various atoms are reported for both hypotheses in Table II (*3*, *15*).

The variation of the quadrupole splitting illustrated by Fig. 5 shows that the distribution of Li is mainly responsible for widening and vanishing of the satellites. Table III collects the experimental and calculated second moments for the various compositions investigated. The composition $Li_{0.70}Mg_{0.15}TaO_3$ fits H1 and composition $Li_{0.50}Zn_{0.25}TaO_3$ rather than H2, but it was impossible to formulate a preference for $Li_{0.95}$

TABLE II

POSITION OF EACH ATOM IN H1 AND H2

Atom	H1			H2		
	x	y	z	x	y	z
Li[a]	0	0	0.2783	0	0	0.2783
Ta[a]	0	0	0	0	0	0
O[a]	0.0498	0.3436	0.0688	0.0498	0.3436	0.0688
$\frac{1}{3}$ Mg (or Zn)	0	0	0.2783	0	0	0.2783
$\frac{1}{3}$ Mg (or Zn)	0	0	0	0	0	0
$\frac{1}{3}$ Mg (or Zn)	0[b]	0[b]	0.1521[b]	0.0498[b]	0.3436[b]	0.1799[b]

[a] Refs. (3, 15).
[b] Octahedral vacancies.

$Mg_{0.15}Ta_{0.95}O_3$ and $Li_{0.95}Zn_{0.15}Ta_{0.95}O_3$. For these two compositions we have thus calculated the electric field gradient in the Li sites for the two hypotheses and compared its value with the experimental one.

Electric Field Gradient Calculation

The ^7Li satellites are observed for the three compositions $LiTaO_3$, $Li_{0.95}Mg_{0.15}Ta_{0.95}O_3$, and $Li_{0.95}Zn_{0.15}Ta_{0.95}O_3$. Their respective experimental quadrupole splittings $\nu_{Q_{exp}}$ are given in Table IV. These values can be connected to the structural results by calculating the electric field gradient (EFG) tensor at the lithium site for each hypothesis (*16*):

For ^7Li ($I = \frac{3}{2}$) the strength of the quadrupole interaction (*17*) can be measured as

$$\nu_Q = 3eV_{zz}Q/2I(I-1)h, \qquad (1)$$

where Q is the ^7Li nuclear quadrupole moment and V_{zz} is the main component of the EFG tensor. The powder spectrum only allows to measurement of the product $\nu_m = \nu_Q(1-\eta)$, where η is the asymmetry parameters defined as

$$\eta = (V_{xx} - V_{yy})/V_{zz}$$

with $0 \leq \eta \leq 1$ according to the usual definition

$$|V_{zz}| \geq |V_{yy}| \geq |V_{xx}|.$$

An axial symmetry of the Li sites (like in $LiTaO_3$) implies $\eta = 0$.

In ionic crystals the main contribution to the field gradient results from the lattice, i.e., from the arrangement of the ionic charges around a given site. The nine (five independent) components of the EFG tensor can be calculated from the relation

$$V_{ij} = \sum_k q_k \sum_i \sum_j (3r_{ik}r_{jk} - \delta_{ij}r_k)/r_k,$$

where $i, j = x, y, z$. $\delta_{ij} = 1$ if $i = j$ and 0 in all other cases. r_{xk}, r_{yk}, and r_{zk} are the coordinates in an arbitrary orthogonal system of the kth atom with charge q_k situated at a distance r_k from the reference site. The calculations have been performed with a computer program established by Pannetier and co-workers (*16*).

TABLE III

COMPARISON OF THE EXPERIMENTAL AND CALCULATED SECOND MOMENTS

Formula	$M_{2_{exp}}(G^2)$	$M_{2_{calc}}(G^2)$ H1	$M_{2_{calc}}(G^2)$ H2	Retained hypothesis
$LiTaO_3$	1.25 (2)	—	—	—
$Li_{0.95}Mg_{0.15}Ta_{0.95}O_3$	1.19 (1)	1.20	1.20	
$Li_{0.70}Mg_{0.15}TaO_3$	1.00 (1)	0.99	1.06	H1
$Li_{0.95}Zn_{0.15}Ta_{0.95}O_3$	1.20 (1)	1.19	1.19	
$Li_{0.50}Zn_{0.25}TaO_3$	0.84 (1)	0.82	0.83	H2

TABLE IV

COMPOSITION, EXPERIMENTAL QUADRUPOLE SPLITTING ($\nu_{Q_{exp}}$), CATIONIC LOCALIZATION, IONIC NET CHARGES, HYPOTHESIS, ASYMMETRY FACTOR (η), ELECTRIC FIELD GRADIENT COMPONENT V_{zz}, AND THEORETICAL EXPERIMENTAL RATIO R (SEE TEXT)

Compositions	$\nu_{Q_{exp}}$ (kHz)	Hypothesis	Net charges Li	Ta	Mg, Zn	O	η	V_{zz}	R_{th}	R_{exp}	Retained, hypothesis
$LiTaO_3$	40.5 ± 0.2	—	1	1.21	—	−0.74	0	0.0697	1	1	—
$Li_{0.95}Mg_{0.15}Ta_{0.95}O_3$	43.4 ± 0.6	H1	1	1.21	0.3	−0.715	0	0.0724	0.963	0.93 ± 0.2	H1
			1	**1.21**	**0.4**	**−0.72**	**0**	**0.0744**	**0.931**		
			1	1.21	0.5	−0.725	0	0.0764	0.912		
		H2	1	1.21	0.3	−0.71	0	0.0675	1.032		
			1	1.21	0.4	−0.72	0	0.0679	1.026		
			1	1.21	1.4	−0.77	0	0.0721	0.966		
			1	1.21	1.6	−0.78	0	0.0729	0.955		
			1	1.21	1.8	−0.79	0	0.0738	0.944		
			1	1.21	2.0	−0.80	0	0.0746	0.934		
$Li_{0.95}Zn_{0.15}Ta_{0.95}O_3$	38.8 ± 0.4	H1	1	1.21	0.4	−0.72	0	0.0744	0.937	1.04 ± 0.01	H2
		H2	1	1.21	0.1	−0.705	0	0.0667	1.045		
			1	**1.21**	**0.2**	**−0.71**	**0**	**0.0671**	**1.038**		
			1	**1.21**	**0.3**	**−0.715**	**0**	**0.0675**	**1.032**		
			1	1.21	0.4	−0.72	0	0.0679	1.026		
			1	1.21	0.5	−0.725	0	0.0683	1.020		

Note. The values for each retained hypothesis are boldface.

The phases are considered ionic crystals. The hypothesis of onefold positively charge lithium is reasonable and supported by previous investigations on crystals of $LiNbO_3$ and $LiTaO_3$ (*15*). The values determined by these authors have been used for the field gradient calculations. The charge distribution in $LiTaO_3$ between Ta and O is illustrated by Fig. 6. The strong covalent bond between tantalum and oxygen leads to net charges 1.21 for tantalum and −0.74 for oxygen.

Magnesium and zinc charges have not really been fixed but several authors assume also an appreciable covalency between magnesium (or zinc) and oxygen (stronger indeed for zinc than for magnesium). Values of electronic density have been determined for the metal–oxygen bond by X-ray Fourier analysis and molecular orbital calculations (*18*). A connection between metal–oxygen distance and valence bond (*19*) allowed us to propose an approximate net charge 0.4 for magnesium and zinc. Nevertheless the EFG calculations have been performed for values in the range 0.3–2.0 for magnesium and 0.1–0.5 for zinc in order to fit on the experimental values.

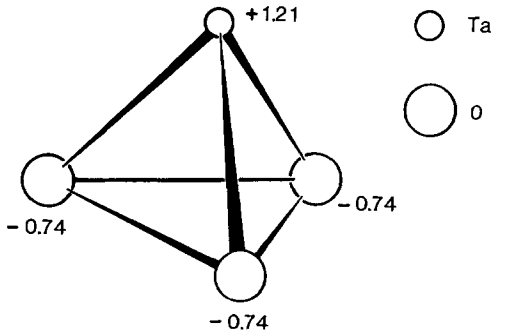

FIG. 6. Charge distribution for $LiTaO_3$ as determined from the field gradient calculations (Ref. (*15*)).

To eliminate the ^7Li quadrupole moment Q for which no accurate value is available, the $R_{exp} = \nu_Q(LiTaO_3)/\nu_Q(S.S.)$ ratio has been determined. ν_Q ($LiTaO_3$) is linked to the ^7Li quadrupole splitting in pure $LiTaO_3$ and ν_Q(S.S.) to the investigated solid solution composition. Theoretical calculations of $R_{th} = V_{zz}(LiTaO_3)/V_{zz}(S.S.)$ have been performed for both hypotheses and for various net charges, they have been compared to $R_{exp} = V_{zz}(LiTaO_3)/V_{zz}(S.S.)$ obtained from Eq. (1) type measurements.

Figures 7 and 8 represent variations of R_{th} with the net charges on magnesium and zinc. A good agreement is observed with experimental value of R_{exp} for a net charge of 0.4 for magnesium in octahedral sites and of about 0.3 for zinc in tetrahedral sites (Table IV). On the contrary H2 for magnesium (Mg in tetrahedral sites), which agrees with a net charge 2+ on magnesium, is unrealistic.

Conclusion

^7Li NMR (quadrupole spectrum evolution) confirmed clearly the strong influence of the cation distribution on the ferroelectric properties of $LiTaO_3$-related phases. A comparison between the experimental and theoretical second moments of $Li_{0.70}Mg_{0.15}TaO_3$ allowed us to localize Mg in octahedral sites (substituting Li or Ta or occupying octahedral vacancies). In $Li_{0.50}Zn_{0.25}TaO_3$ zinc partially substitutes for Li and Ta in their octahedral sites, while the remaining part seems to occupy statistically tetrahedral vacancies.

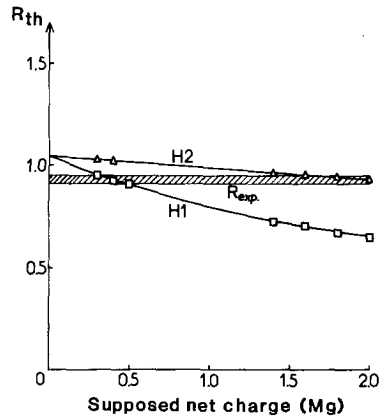

FIG. 7. Variation of R_{th} with the net charge on magnesium for the composition $Li_{0.95}Zn_{0.15}Ta_{0.95}O_3$.

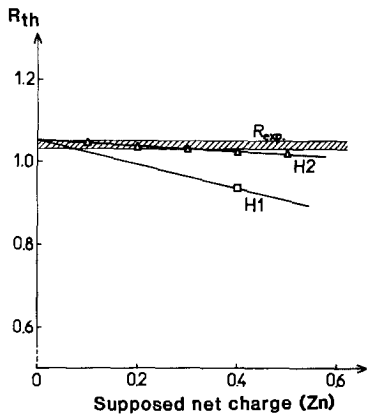

FIG. 8. Variation of R_{th} with the net charge on zinc for the composition $Li_{0.95}Zn_{0.15}Ta_{0.95}O_3$.

EFG calculations allowed analogous distributions for $Li_{0.95}Mg_{0.15}Ta_{0.95}O_3$ and $Li_{0.95}Zn_{0.15}Ta_{0.95}O_3$ to be proposed: Mg occupies only octahedral sites and vacancies while a part of zinc appears to be localized in tetrahedral vacancies.

It is not easy to correlate the t_C evolution to the substitution mechanism. Let us compare various solid solutions where vacant octahedral sites are occupied by the substituting atoms: Li in $Li_{1+x}Ta_{1-x/5}O_3$ (*10*), Mg in $Li_{1-x}Mg_{3x}Ta_{1-x}O_3$, Ti in $Li_{1-x}Ti_xTa_{1-x}O_3$ ($x \leq 0.075$) (*10*), Zr in $Li_{1+x}Zr_xTa_{1-x}O_3$ (*20*).

One observes an increase of t_C, i.e., a stronger value of the polarization vector $\mathbf{P}_s$, for Li and Mg, the electropositivity of which exceeds that of Ta. On the contrary a t_C decrease is detected when the electropositivity becomes weaker (Ti, Zr).

As far as tetrahedral vacancies are partially occupied by substituting atoms (Li in $Li_{1+x}Ti_xTa_{1-x}O_3$ ($x > 0.075$), Zn in $Li_{1-x}Zn_{3x}Ta_{1-x}O_3$), the corresponding effect

seems to be competition against the influence of electropositivity in octahedral sites. In the case of zinc it results in a clear t_C decrease.

Our next goal will be now to improve the calculation of spontaneous polarization and Curie temperature, taking into account all atomic positions.

Acknowledgment

The authors thank Dr. J. Pannetier (Ill Grenoble, France) who provided them with the EFG calculation program.

References

1. J. RAVEZ AND F. MICHERON, *Actual. Chim.* **1,** 9 (1979).
2. S. C. ABRAHAMS AND J. L. BERNSTEIN, *J. Phys. Chem. Solids* **28,** 1685 (1967).
3. S. C. ABRAHAMS, W. C. HAMILTON, AND A. SEQUEIRA, *J. Phys. Chem. Solids* **28,** 1693 (1967).
4. R. R. NEURGAONKAR, T. C. LIM, AND L. E. CROSS, *Ferroelectrics* **27,** 63 (1980).
5. Y. TORII, T. SEKIYA, Y. YAMAMOTO, K. KOYABAHSI, AND Y. ABE, *Mater. Res. Bull.* **18,** 1569 (1983).
6. G. -T. JOO, J. RAVEZ, AND P. HAGENMULLER, *Rev. Chim. Miner.* **22,** 18 (1985).
7. B. ELOUADI, M. ZRIOUIL, J. RAVEZ, AND P. HAGENMULLER, *Ferroelectrics* **38,** 793 (1981).
8. G. -T. JOO, J. RAVEZ, AND P. HAGENMULLER, *Ferroelectr. Lett. Sect.* **4,** 73 (1985).
9. J. RAVEZ, G. -T. JOO, J. SENEGAS, AND P. HAGENMULLER, *Japan J. Appl. Phys.* **24,** (Suppl. 2), 1000 (1985).
10. M. ZRIOUIL, J. SENEGAS, B. ELOUADI, AND J. B. GOODENOUGH, *Mater. Res. Bull.* **20,** 679 (1985).
11. G. -T. JOO, J. RAVEZ, AND P. HAGENMULLER, *Rev. Chim. Miner.* **23,** 20 (1986).
12. E. R. ANDREW, *Phys. Rev.* **91,** 425 (1953).
13. J. H. VAN VLECK, *Phys. Rev.* **74,** 1168 (1948).
14. A. ABRAGAM, "Les Principes du Magnétisme Nucléaire," Chap. IV, p. 136, Presse Univ. France, Paris (1961).
15. G. E. PETERSON AND P. M. BRIDENBAUCH, *J. Chem. Phys.* **48,** 3402 (1968).
16. J. -M. CRETTEZ, E. COQUET, J. PANNETIER, J. BOUILLOT, AND M. DURAND-LEFLOCH, *J. Solid State Chem.* **56,** 133 (1985).
17. M. H. COHEN AND F. REIF, *in* "Solid State Physics" (F. Seitz and D. Turnbull, Eds.), Vol. 5, p. 321, Academic Press, New York (1957).
18. P. J. DURRANT AND B. DURRANT, *in* "Advanced Inorganic Chemistry" (W. Clowes, Ed.), p. 443. Longmans, Green, NY (1966).
19. I. D. BROWN, *in* "Structure and Bonding in Crystals" (M. O'Keeffee and A. Navrotsky, Eds.), Vol. II, p. 1, Academic Press, Orlando, FL (1981).
20. M. ZRIOUIL, B. ELOUADI, J. RAVEZ, AND P. HAGENMULLER, *J. Solid State Chem.* **51,** 53 (1984).